A ∼6 Ma chemical weathering history, the grain size dependence of chemical weathering intensity, and its implications for provenance change of the Chinese loess–red clay deposit

Shangfa Xiong*, Zhongli Ding, Yuanjian Zhu, Ru Zhou, Haijian Lu

Key Laboratory of Cenozoic Geology and Environment, Institute of Geology & Geophysics, Chinese Academy of Sciences, 100029 Beijing, China

ARTICLE INFO

ABSTRACT

Major element chemical analyses of the Baishui loess–red clay sequence (35° 24′ 10″N, 106° 54′ 43″E, Gansu Province, China) reveal that, the chemical weathering intensities inferred from CIA (chemical index of alteration) values have progressively weakened and increased in amplitude with decreasing age. The general trend of the CIA can be correlated well with the oxygen isotope variations of the deep sea sediments. Analyses of multiple size fractions (<5 μm, 5–20 μm and 20–63 μm) indicate that the CIA and the major element abundances are strongly grain size dependent. The chemical alternation of all three size fractions is relatively weak, and the long-term variation in chemical composition of the loess–red clay is mainly controlled by the mixing of fresh detritus from different source areas. The CIA variability of the coarse fractions (5–20 μm and 20–63 μm) within the section is apparently different from that of the fine fraction (<5 μm), implying a different erosion–transportation–deposition–weathering history. From 1 Ma onward, CIA values for all size fractions decrease, indicating an increasing input of fresh or poorly weathered detritus in the desert source regions of loess deposits. Sequential variations in the K_2O/Al_2O_3, Na_2O/Al_2O_3, CaO/Al_2O_3 and MgO/Al_2O_3 ratios from 4.5 Ma to about 0.6 Ma in bulk and size fractioned samples may reflect provenance change as well as changing chemical weathering processes.

© 2010 Elsevier Ltd. All rights reserved.

1. Introduction

The Late Cenozoic has witnessed progressive environmental change ultimately leading to the major expansion of northern hemisphere glaciation at about 2.7 Ma (e.g., Raymo, 1994; Shackleton et al., 1995; Maslin et al., 1996; Zachos et al., 2001). The extensive and continuous loess–red clay eolian deposits in northern China, with some sections as old as 20 Ma (e.g., Guo et al., 2002), are an important marker of this Late Cenozoic environmental transition (e.g., Liu et al., 1985; Ding et al., 1994). The Chinese loess–red clay archived continental-scale climatic and environmental changes during the Pliocene through Pleistocene (e. g., Ding et al., 1994; Ding et al., 1999, 2001a), including provenance and chemical weathering variations over time (e.g., Liu et al., 1985; Gallet et al., 1996; Chen et al., 2007). In the past two decades, extensive studies of the chemistry of the Chinese loess–red clay deposits have been conducted and several common concepts have emerged:

(1) Early works (e.g., Liu et al., 1985; Wen et al., 1989; Liu et al., 1993; Gallet et al., 1996) centered on the general uniformity of the chemical (isotopic, major and trace elements) composition of Chinese loess, and it is commonly accepted that the loess sources must be the result of multiple cycles of weathering, erosion, transport and deposition of crustal material (Liu et al., 1985; Jahn et al., 2001). Loess has been used as an example of the average composition of the UCC (upper continental crust) in some models (Taylor et al., 1983; Wen et al., 1989; Liu et al., 1993; Gallet et al., 1996, 1998). More recently, research has been focused on finding tracers of different loess source regions (e.g., Sun, 2002; Yokoo et al., 2004; Nakano et al., 2004; Chen et al., 2007; Sun et al., 2007; Yang et al., 2007), and several potential source regions for loess and modern eolian dust have been identified by correlating isotopic and REE (rare earth elements) characteristics between atmospheric dust, eolian deposits and desert sediments.

(2) Systematic variations in chemical composition between the loess and interbedded palaesols suggest that chemical weathering and associated pedogenic processes may have altered the original chemical composition of the loess–red clay deposit over time (Liu et al., 1985; Gallet et al., 1996; Chen et al., 1999;

Guo et al., 2000), although it is still not clear to what extent provenance changes may have contributed to the variations in the composition of the loess and interbedded palaesols.

(3) The long-term geochemical evolution of the loess−red clay has been attributed to variation in chemical weathering intensity within the loess−red clay sequence (e.g., Liu et al., 1985; Wen et al., 1989; Gu et al., 1999; Ding et al., 2001b; Yang et al., 2006). However, this long-term geochemical evolution may also signal provenance changes. For example, the remarkable changes in Nd and Sr isotopes were observed in the loess−red clay sequence and may indicate a temporal variation in loess provenance (Sun, 2005).

The loess−red clay deposits of northern China have undergone extensive sediment recycling, mixing, and particle sorting processes before deposition and subsequent pedogenic alteration (e.g., Liu et al., 1985; Smalley, 1995; Wright, 2001), thus the chemical composition of the loess−red clay should retain a complex signal reflecting the interaction and overprinting of these processes. For further understanding of the provenance, paleoclimatic and tectonic implications of the loess−red clay chemistry, it is necessary to differentiate between the relative contributions of these processes. This has proven to be a difficult task and much work remains to be done.

One important issue to address is the grain size dependence of major element chemical composition used to generate chemical weathering intensity estimates in the loess−red clay deposits. Previous studies have shown that the chemical composition of different grain size fractions of sediment differs markedly (e.g., Yang et al., 2006) due to the natural variation in particle composition with grain size, with clay minerals dominating the fine fraction and primary minerals such as quartz and plagioclase as well as rock fragments more common in the coarse fraction. Thus the bulk chemical composition of the loess−red clay sequence is strongly influenced by the grain size, and grain size is also influenced by chemical weathering intensity, provenance and transport process changes. One approach is to use proxies independent of grain size (e.g., Yang et al., 2006), while another possible approach is to study the chemical composition of different size fractions, in order to minimize the effect of grain size on the chemical composition of the loess−red clay.

Here we separated the loess−red clay samples into three size fractions (<5 μm, 5−20 μm and 20−63 μm) and analyzed the chemical composition of bulk samples and these 3 different size fractions for the loess−red clay sequence of the Baishui section, in the Chinese Loess Plateau (Fig. 1). This study enables us to reveal the systematic differences in chemical composition for the different size fractions, and to investigate compositional variations as well as the inferred chemical weathering history of the different size fractions for the loess−red clay sequence.

2. Material and methods

The Baishui section (35° 24′ 10″N, 106° 56′43″E) is located in the northwest part of the central Loess Plateau, 30 km southeast of Pingliang City, Province Gansu (Fig. 1). This section contains an upper 214 m alternating loess−paleosol sequence and a lower 79.2 m relatively uniform red clay deposit, with the most-developed soils in the upper unit being S1, S3, S4, S5 and S32, while the thickest loess layers are L9, L15, L24, L27 and L33. The couplets of loess and soil in the Baishui section are identical in pattern to the sections (e.g., Lingtai section; Ding et al., 1999) developed in the middle part of the Loess Plateau, but the pedogenic characteristics (e.g., color, abundance in translocated clay skins and Fe−Mn films) indicate a less developed soils than the Lingtai section. The age control of the Baishui section was generated by correlating the magnetic susceptibility record with the Jingchuan record, in which the age control points were based on the magnetic reversal stratigraphy (Ding et al., 2001a). The base of the red clay in the Baishui section is about 6.2 Ma old (Xiong et al., 2003). The magnetic susceptibility of the Baishui section was measured at an interval of 10 cm with a Bartington MS2 susceptibility meter using air-dried samples (Xiong et al., 2002), and the grain size distribution was determined with a Sald-3001 diffraction particle analyzer after the carbonate-free samples had been ultrasonically treated in a 20% $(NaPO_3)_6$ solution (Xiong et al., 2003).

We have analyzed the chemical composition of bulk samples at about a 1-m interval, and size-fractionated samples at about a 2-m interval for the loess−red clay sequence of Baishui section. Three size fractions (<5 μm, 5−20 μm and 20−63 μm) of the loess−red clay were separated by using a sedimentation method. Carbonate and organic carbon were removed respectively by using 1 M acetic

Fig. 1. Map of the Chinese Loess Plateau and adjacent regions showing locations of the Baishui, Lingtai and Jingchuan sections (image from the Google Earth).
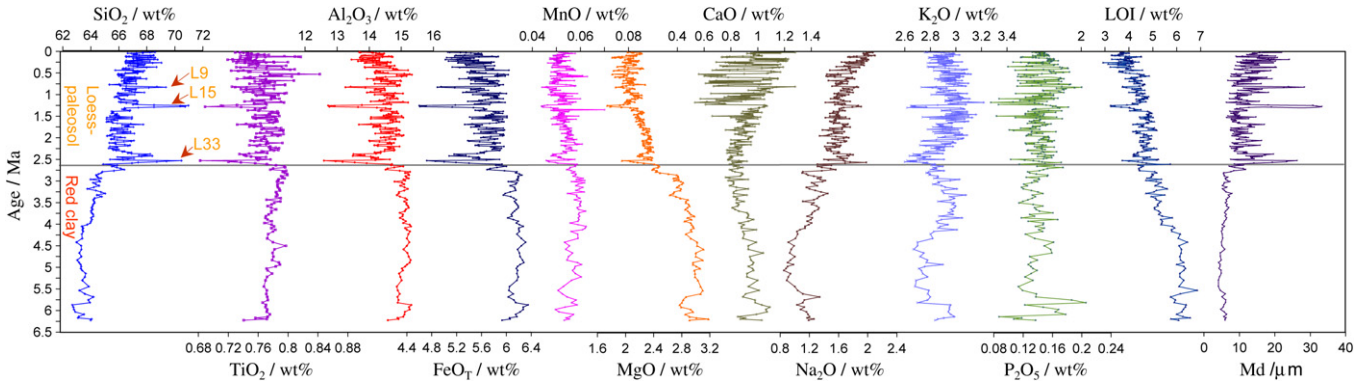
Fig. 2. Variation of bulk major element concentrations as well as the LOI (Loss on Ignition) and Md (Medium Grain Size) in the Baishui loess−red clay sequence. The boundary of loess−paleosol and red clay and loess L9, L15, L33 are also indicated.

acid and 30% H_2O_2 for the bulk and size-fractionated samples. About 0.6 g of ground sample was heated to 1000 °C in a muffle furnace, measuring the weight loss, and then mixed with 6 g of $Li_2B_4O_7$ followed by heating to 1100 °C in a Pt crucible and followed by cooling as a glass disc. The prepared discs were measured on a Shimadzu XRF-1500 for major element concentrations. Four standard samples (GSS, Geochemical Standard Reference Sample Soils, Institute of Geology and Geophysics, Chinese Academy of Sciences) were used for quality control of the measurements. Analytical uncertainties are ±2% for all major oxides except P_2O_5 and MnO for which uncertainties can be up to ±10%.

3. Results

### 3.1. Bulk chemical composition and chemical weathering intensity

Major element analysis for the bulk samples (Fig. 2) shows that the major difference in composition appears between the loess and the underlying red clay, especially in weight percent of SiO_2, Al_2O_3, TiO_2, FeO_T, MgO and Na_2O. For example, the proportion of SiO_2 is obviously larger in the loess, whereas the weight percentages of Al_2O_3, TiO_2 and FeO_T are larger in the red clay (Fig. 2). This difference in composition is mainly influenced by the grain size, with enriched Al_2O_3, TiO_2, FeO_T and MgO and depleted SiO_2 and Na_2O values in fine-grained, clay mineral rich samples. The compositional difference between the quartz-rich loess and clay-rich paleosol is also apparent (Fig. 2).

In a Harker diagram (Rollinson, 1993) for the bulk samples from the Baishui loess−red clay section, the samples seem to fall segmented trends (Fig. 3). The slope of the lines for the red clay samples (<65% SiO_2) is different from that of the loess−paleosol samples (>65% SiO_2), implying different sources. The loess and red clay samples in an A−CN−K triangle plot show a line parallel to Nesbitt's weathering trend (Nesbitt et al., 1996) (Fig. 4), with the red clay samples exhibiting more intensive weathering than the loess. The corresponding CIA (Chemical Index of Alteration) (Nesbitt and Young, 1982) is about 61−71, suggesting intermediate (CIA = 60−80) chemical weathering intensity. It is notable that in the A−CN−K plot the loess and red clay samples follow a similar but different trend line, indicating a variation in detrital provenance for the loess and red clay deposits.

There are many weathering indices proposed in previous studies (Table 1), and using these indices we calculated the chemical weathering intensities from the Baishui loess−red clay deposit (Fig. 5). It is apparent that different indices display different patterns. In general, the CIA, CIW (Chemical Index of Weathering) and WI (Weathering Index) indices exhibit similar trends with decreasing values (indicating less weathering) and larger amplitudes towards the top of the section. Ruxton's (1968) simple proxy of aluminium over silica (R, Ruxton ratio) shows a pattern mimicking the median grain size, with higher values of R, indicative of intensified weathering, corresponding to finer samples. The weathering indices V (Vogt ratio), WR (Weathering ratio) and MWPI (Modified Weathering Potential Index) display a third type of trend, with a similar variation with CIA in the upper part of the sequence (from ∼1.2 Ma to present) but a different pattern in the
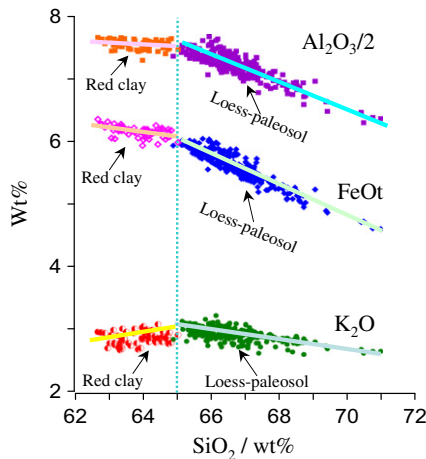
Fig. 3. Bivariate plots of the Al_2O_3, FeOt, K_2O versus SiO_2 (Harker diagram) in bulk samples for the loess−paleosol and red clay samples of the Baishui section.
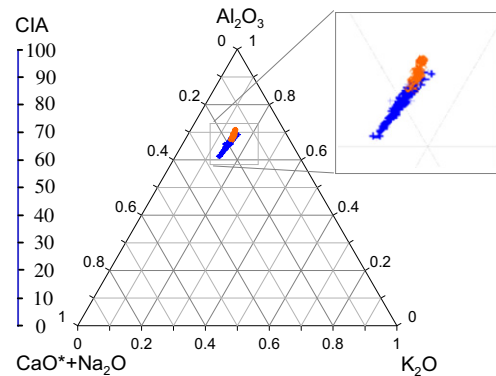
Fig. 4. Baishui loess−paleosol (blue) and red clay (orange) bulk compositions plotted in A−CN−K diagram. (For interpretation of the references to colour in this figure legend, the reader is referred to the web version of this article.)

Table 1
Summary of weathering indices in this study (using molecular proportions).

$CIA = [Al_2O_3/(Al_2O_3 + CaO^* + Na_2O + K_2O)] \times 100$	(Nesbitt & Young, 1982)
$CIW = [Al_2O_3/(Al_2O_3 + CaO^* + Na_2O)] \times 100$	(Harnois, 1988)
$WI = [(2Na_2O/0.35) + (MgO/0.9) + (2K_2O/0.25) + (CaO^*/0.7)] \times 100$	(Parker, 1970)
$V = (Al_2O_3 + K_2O)/(MgO + CaO^* + Na_2O)$	(Vogt, 1927)
$WR = [(CaO^* + MgO + Na_2O)/ZrO_2 \text{ or } TiO_2]$	(Chittleborough, 1991)
$MWPI = [(Na_2O + K_2O + CaO^* + MgO)/(Na_2O + K_2O + CaO^* + MgO + SiO_2 + Al_2O_3 + Fe_2O_3)] \times 100$	(Vogel, 1975)
$R = SiO_2/Al_2O_3$	(Ruxton, 1968)

Where CaO^* is the amount of CaO incorporated in the silicate fraction of the sample.

lower part of the loess–paleosol and the red clay deposit. The weathering intensities of the red clay (from 6.2 to 2.7 Ma) revealed by the weathering indices of V, WR and MWPI are apparently lower than that of paleosols in the upper section or even similar to that of the loess deposit, in contrast with the conclusions by field observations that the red clay sequence has stronger pedogenic intensity than that of the Holocene paleosol (e.g., Ding et al., 1999). Thus it appears that V, WR and MWPI are not appropriate indices in revealing chemical weathering intensity for the whole sequence of the loess–red clay deposit.

It seems that CIA and CIW curves follow the trend of the oxygen isotope records of deep ocean sediment (Mix et al., 1995; Shackleton et al., 1995) (Fig. 5). The chemical weathering indices exhibit no clear correlation with the magnetic susceptibility of the loess–red clay, but most of the indices display similar patterns to the variation of grain size (Fig. 6), suggesting the dependence of these indices on grain size.

### 3.2. Chemical weathering intensity of size fractions

The chemical compositions of the size fractions (<5 μm, fine; 5–20 μm, intermediate and 20–63 μm, coarse) show systematic differences in major element content and chemical weathering intensity (Figs. 7 and 8). The A–CN–K triangle plot reveals three groups corresponding to the 3 different size fractions, with finer grains tending to have a higher weathering intensity (Fig. 7). It seems that the major elements have different distribution patterns in each size fraction (Fig. 8). For example, the coarse fraction has the highest SiO_2 and NaO_2 concentration, while the highest Al_2O_3, FeO_T,

MgO and K_2O concentration is in the fine fraction. The concentration of TiO_2 in the intermediate fraction (5–20 μm) is higher than those in the coarse and fine fractions.

The CIA values for different size fractions yield a pattern of strong grain size dependence (Fig. 9), with a systematic change in CIA value from about 55–60 for the coarse fraction (20–63 μm) through 57.5–67.5 for the intermediate fraction (5–20 μm) to about 70–80 for the fine fraction (<5 μm). The CIA of the coarse fraction has a similar sequential variation pattern with that of the intermediate fraction, exhibiting several megacycles superimposed on more frequent fluctuations. The fine fraction exhibits different CIA variation compared with the coarser fractions. From 6 Ma to about 1 Ma, the CIA values of the fine fraction fluctuate over a narrow range around 77, and from 1 Ma onward, the CIA values display a decreasing trend with greatly amplified variations, indicating an overall weakened chemical weathering intensity, but higher chemical weathering variability towards the upper part of the loess–paleosol section.

3.3. Chemical evolutions of the size fractions

The incipient (CIA = 50–60) to intermediate (CIA = 60–80) chemical weathering intensity reflects that the loess–red clay deposit has been experiencing the removal of labile cations (mainly Mg^{2+}, Ca^{2+}, Na^+ and K^+) relative to stable residual constituents (Al^{3+}, Ti^{4+}). Figs. 10 and 11 illustrate the sequential variations in MgO/Al_2O_3, CaO/Al_2O_3, Na_2O/Al_2O_3 and K_2O/Al_2O_3 ratios for the bulk and the different size fractions. The bulk and fine fraction
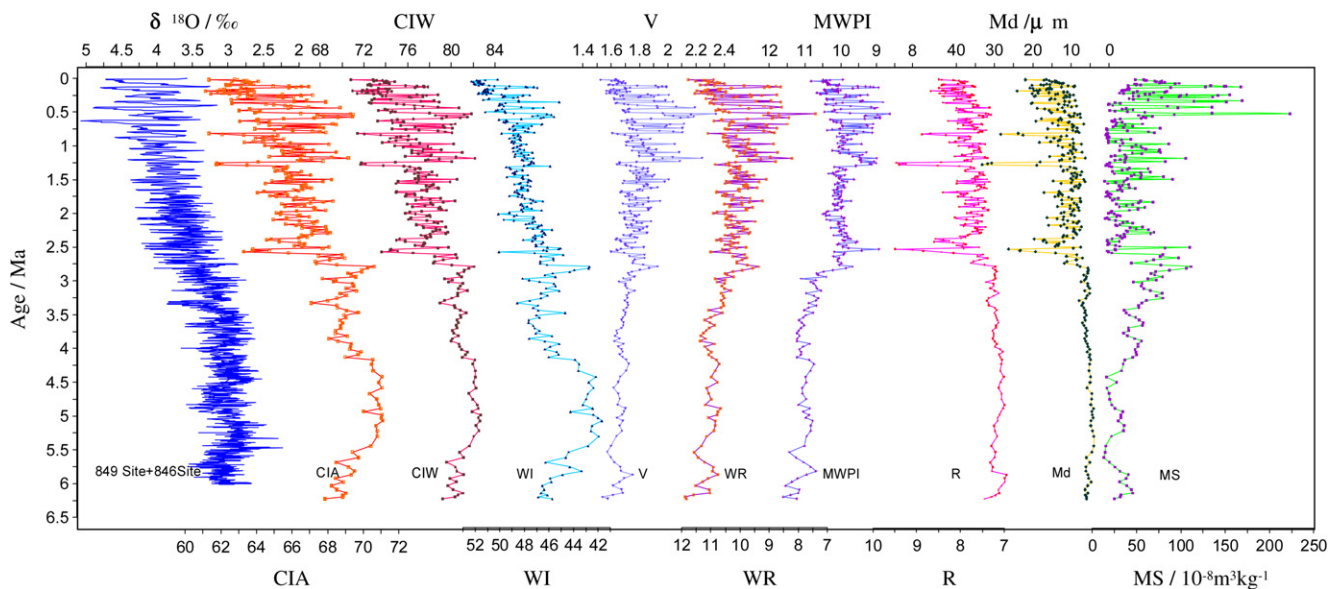

Fig. 5. $\delta^{18}O$ record of deep sea sediment (Mix et al., 1995; Shackleton et al., 1995) and variations of the chemical weathering ratios, median grain size (Md) and magnetic susceptibility (MS) in the Baishui loess–red clay section.
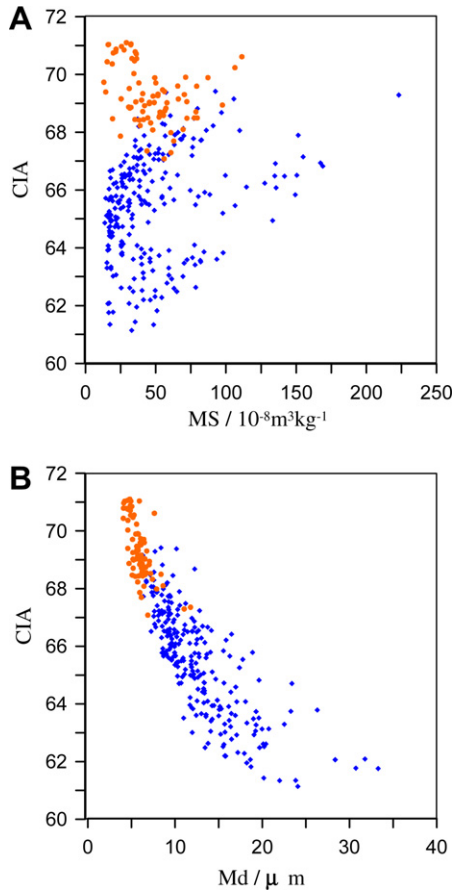
Fig. 6. Diagrams of (A) CIA versus MS and (B) CIA versus Md for samples of the Baishui section (Orange dot: red clay; Blue diamond: loess–paleosol). (For interpretation of the references to colour in this figure legend, the reader is referred to the web version of this article.)

samples display similar temporal evolutions. The lowest ratio values seem to occur progressively from about 5.5–4.5 Ma for Na_2O/Al_2O_3 and K_2O/Al_2O_3 ratios to about 2.5 Ma for CaO/Al_2O_3 ratio and about 0.6 Ma for MgO/Al_2O_3 ratio (Fig. 10). For each pair of fluctuations in CaO/Al_2O_3 ratio, the higher and lower value ends correspond to loess or poorly developed red clay layers and
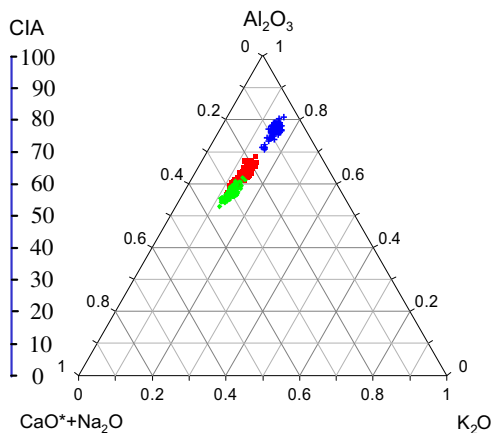
Fig. 7. Geochemical compositions of size fractions of the Baishui section plotted in the A–CN–K diagram (Blue: <5 μm; Red: 5–20 μm; Green: 20–63 μm). (For interpretation of the references to colour in this figure legend, the reader is referred to the web version of this article.)

paleosols or well-developed red clay layers, respectively. The MgO/Al_2O_3 ratio has decreased steadily from red clay through loess–paleosol deposit, but from about 0.6 Ma a transition to increasing values occurs. From about 0.6 Ma, steeper increases in MgO/Al_2O_3, Na_2O/Al_2O_3 and K_2O/Al_2O_3 ratios toward the present were observed.

For the coarse (20–63 μm) and intermediate (5–20 μm) fractions rather different trends are revealed. There is no low K_2O/Al_2O_3 ratio at about 5.5–4.5 Ma. However, a shift at about 5.5–4.5 Ma for Na_2O/Al_2O_3 ratio and at about 2.5 Ma for CaO/Al_2O_3 ratio is still observed (Fig. 11). From about 0.6 Ma, a decease in the K_2O/Al_2O_3 ratio and increases in the other ratios can be seen for the coarse and intermediate fractions (Fig. 11).

4. Discussion

4.1. Sequential variation and grain size dependence of chemical weathering intensity for the loess–red clay deposit

The chemical composition of the loess deposits can be used to infer chemical weathering intensity and/or provenance changes. The differences in the chemical compositions between loess and paleosols and the long-term chemical evolution of the sediments are important for understanding the regional climate and provenance changes on orbital and tectonic timescales. In the past several decades, much work has been done on the chemical composition of the Chinese loess–paleosol sequences on different temporal scales (e.g., Liu et al. 1965, 1966; Wen et al., 1989; Gallet et al., 1996; Chen et al., 1999; Gu et al., 1999; Guo et al., 2000; Jahn et al., 2001; Ding et al., 2001b, 2001c; Yang et al., 2006).

Gallet et al. (1996) analyzed the chemical composition of the Luochuan sequence in the Loess Plateau, and found that Ca, Rb, Sr, U and Ce are strongly fractionated between the loess and paleosols during pedogenesis. They concluded that the pattern of elemental variation of the upper part of the Luochuan section is similar to that of the magnetic susceptibility signal. However, this conclusion was modified by their later work (Jahn et al., 2001) where the soil development patterns inferred from chemical indicators at other loess plateau sites seemed to be very different from those of magnetic susceptibility. Based on the low values and small ranges of the CIA estimates, Jahn et al. (2001) suggested that the protolith of loess has only undergone weak weathering before erosion and transport and that the pedogenetic imprint in the middle part of the Loess Plateau in Xifeng is very weak.

A long-term study of the evolution of the loess–paeosols chemistry (Gu et al., 1999) indicated a stepwise increase in the Na/Al ratio at about 5.6 Ma, and proposed that it mainly resulted from changes in chemical composition of the dust in source regions. Ding et al. (2001b) analyzed the ratios of citrate–bicarbonate–dithionite (CBD) extractable Fe_2O_3 to total Fe_2O_3 concentrations (Fe_2O_3 ratio) of the Lingtai sequence. The analysis clearly shows higher values of the Fe_2O_3 ratio in the soil units compared to the loess horizons, implying a higher weathering intensity for soil horizons. The study reveals that there are three time intervals with high Fe_2O_3 ratios within the Lingtai sequence, i.e., 4.8–4.1 Ma, 3.4–2.6 Ma, and during the interglacial periods of the past 0.8 Ma. Yang et al. (2006) used a chemical weathering index, i.e., the $(CaO^* + Na_2O + MgO)/TiO_2$ ratio, for the loess–paleosols, and their analysis shows that the $(CaO^* + Na_2O + MgO)/TiO_2$ ratio of the Lingtai section exhibits relatively regular oscillations with small amplitudes in the early Pleistocene, then the ratio increases rapidly upward with larger amplitudes from 0.85 to 0.6 Ma to the present. The general increase in the ratio indicated a lowered chemical weathering intensity in the dust source regions, according to the authors (Yang et al., 2006). However, the larger amplitudes in chemical weathering intensity
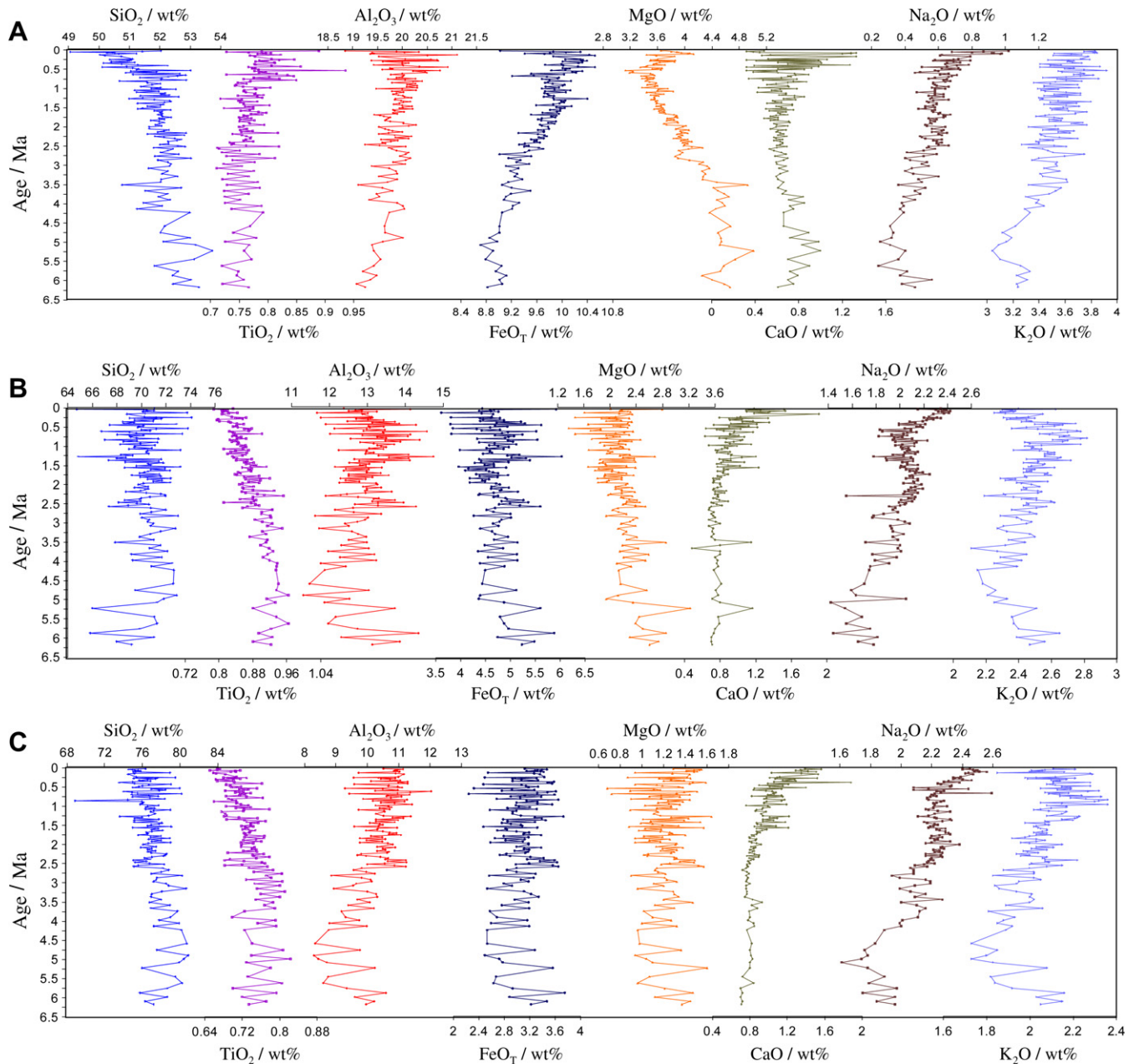
Fig. 8. Variation of major element concentrations for size fractions in the Baishui section (Upper: <5 μm; Middle: 5–20 μm; Lower: 20–63 μm). Mn and P are not shown.

could imply a stronger, rather than the suggested lowered (Yang et al., 2006), chemical weathering intensity in the depositional areas (at least during the interglacial periods).

As revealed by previous work (Gu et al., 1999; Yang et al., 2006), our results also show an upward weakening trend of weathering intensity. The bulk composition analysis of the loess–red clay reveals that the CIA values display a pattern similar to the oxygen isotope record of deep ocean sediment (Fig. 5), with an upward decreasing trend and enlarged amplitudes in younger samples. However, this similarity could be an artifact of the grain size effect on the chemical weathering intensity. It is apparent that the concentration of the major elements and the resulting chemical weathering calculations for the loess–red clay are strongly grain size dependent, and the sequential variations in CIA, CIW, WI and R values have largely mimicked grain size changes (Fig. 5). The weathering indices such as V, WR and MWRI, do not reflect the

actual difference in weathering intensity between the loess–paleosol and red clay which is apparent in field observation and in other proxy studies (e.g., Ding et al., 1999; Gylesjo and Arnold, 2006), and seem inappropriate for depicting chemical weathering intensity for the whole sequence of the loess–red clay deposit. Thus, a more complete picture of the chemical weathering history for the loess–red clay deposit should be sought in the chemistry of size fraction analysis.

The chemistry of three size fractions from the loess–red clay deposits reveals different features than the bulk sample composition (Figs. 8 and 9). As expected, the finer fractions have higher CIA values than the coarser ones, and the sequential CIA value variations for different size fractions also display different patterns, suggesting each size fraction preserves unique information about the loess source material and weathering history. It is observed that the CIA values of the coarse and intermediate fractions (20–63 μm
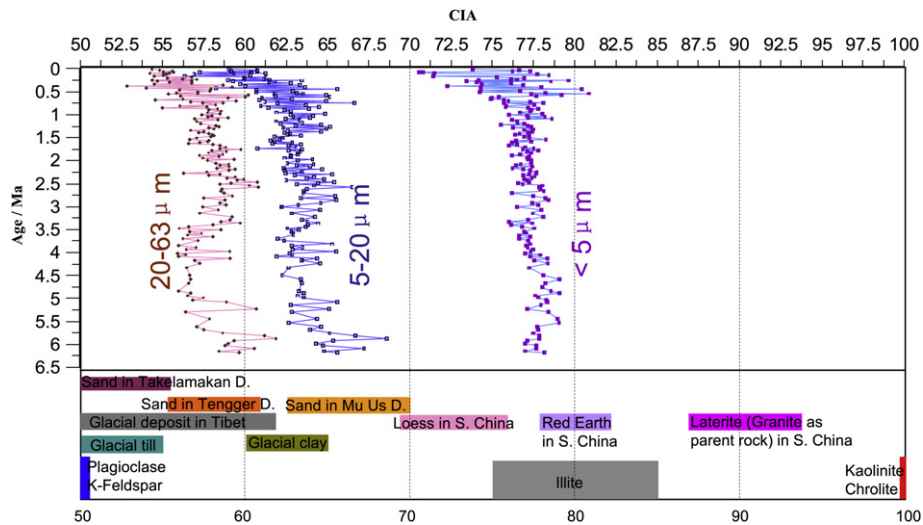
Fig. 9. Variation of CIA for size fractions in the Baishui section. Also shown are CIA value range of some typical minerals (Nesbitt and Young, 1982) and local deposits (Xiong and Li, 1987; Chen et al., 1998; Xiong et al., 2001).

and 5–20 μm, respectively) exhibit several megacycles and decline at about 6–5 Ma, 2.7–1.5 Ma and ∼1.2–1 Ma. The CIA values of the fine fraction (<5 μm) show restricted variation around 77.5 between 6 Ma and 1 Ma followed by a general decreasing trend with amplified fluctuations. The common trend is that from ∼1 Ma, all the three size fractions show an overall declining trend in CIA values.

It seems that the high values of CIA for the fine fraction at about 5.5–4.3 Ma, 3.2–2.7 Ma (Fig. 9) may correlate with the high Fe_2O_3 ratio values at about 4.8–4.1 Ma, 3.4–2.6 Ma through the Lingtai sequence (Ding et al., 2001b). High values of CIA at about 3.2–2.7 Ma can be also observed in the record of coarse and intermediate fractions (Fig. 9), while at bout 5.5–4.3 Ma corresponding values of CIA for coarse and intermediate fractions are relatively low. We cannot give a satisfactory interpretation for this difference in CIA variations between the fine fraction and coarse and intermediate fractions.

The overall declining trend in CIA values from ∼1 Ma is broadly in accordance with the result of Yang et al. (2006), in which the $(CaO^* + Na_2O + MgO)/TiO_2$ ratio increases rapidly upward from 0.85 to 0.6 Ma to the present, implying a lowered chemical weathering intensity. This seems contrary to the findings of Ding et al. (2001b) for Fe_2O_3 ratio of Lingtai, in which the past 0.8 Ma has high Fe_2O_3 ratio values during the interglacial periods. The trend of generally decreasing CIA values during the past 1 Ma in the Baishui section is overprinted with the largest glacial–interglacial CIA amplitude variation and some of the highest CIA values in the record, consistent with the observations of Ding et al. (2001b). Thus the overall declining trend in CIA values for the three size fractions from ∼1 Ma may imply a lowered chemical weathering intensity in the dust source regions (at least during the glacial periods), and the larger variation amplitudes in CIA values may signal stronger weathering intensity in the loess depositional areas, at least during interglacial periods.

This interpretation is also supported by the comparison between the CIA values of loess–red clay and that of the deposits from different environments. The CIA values of the loess–red clay bulk samples indicate an intermediate weathering intensity (CIA = 60–80), however, for the coarse fraction of the loess–red clay, the CIA values are lower and about only 5 units higher than that for glacial till (Nesbitt and Young, 1982) (Fig. 4), and within the CIA value ranges of hill-slope sediments and glacial moraines in the

Tibetean plateau and of dune sands in the Tengger desert (Xiong and Li, 1987) (Fig. 9). The intermediate fraction (5–20 μm) has slightly higher CIA values, similar to those of the glacial clay (Nesbitt and Young, 1982) and dune sands in the Mu Us desert (Chen et al., 1998) (Fig. 9). These lower CIA values for the coarse and intermediate fractions suggest that these fractions of the loess–red clay deposits have experienced only minor chemical alteration after erosion and delivery from the source regions. Although variations in CIA values between loess and paleosols are observed, the amplitudes of variation are small (mostly less than 5), implying minor pedogenic alterations in the overall CIA value changes of the coarse and intermediate fractions.

For the fine fraction (<5 μm), CIA value varied largely in the range of illite (Nesbitt and Young, 1982) (Fig. 9), with smaller variations (less than 2) between less developed and well-developed layers for most intervals of the sequence, and in the upper part of the sequence, the CIA values fluctuated with a larger amplitude (about 5–7) between loess and paleosols. It is estimated that illite concentration is around 50% in <2 μm size fraction at Lingtai (Gylesjo and Arnold, 2006) but the CIA value of the fine fraction also reflects the mixing contribution of less weathered minerals (such as plagioclase and K-feldspar) and well-weathered minerals (such as kaolinite). Clay mineral analyses (Gylesjo and Arnold, 2006) also display small but significant differences in illite (higher in soils) and kaolinite (higher in loess) between loess and paleosols over the last 0.5 Ma, where the greatest amplitudes in CIA at Baishui are also observed. The highest average chlorite and lowest average kaolinite concentration in the loess–paleosol occurred in the last 0.5 Ma at Lingtai. Because chlorite is markedly unstable in pedogenic environments (Dixon and Weed, 1989), increasing chlorite and decreasing kaolinite values after 0.5 Ma suggests that loess–red clay deposit may have experienced only minor chemical weathering during this period. However, higher kaolinite abundance in loess than paleosols could suggest varying source regions, with some kaolinite inherited from older sediments in source area. Extensive Jurrasic, Cretaceous and Paleogene basins are distributed in the source regions of the eolian loess–red clay deposits (Institute of Geology, Chinese Academy of Geological Sciences and Wuhan College of Geology, 1985; Editing Committee of Geological Atlas of China, 2002) (see Fig. 12), and the highly weathered sediments from these uplifted basins could deliver large amounts of strongly weathered minerals (such as kaolinite). Thus it
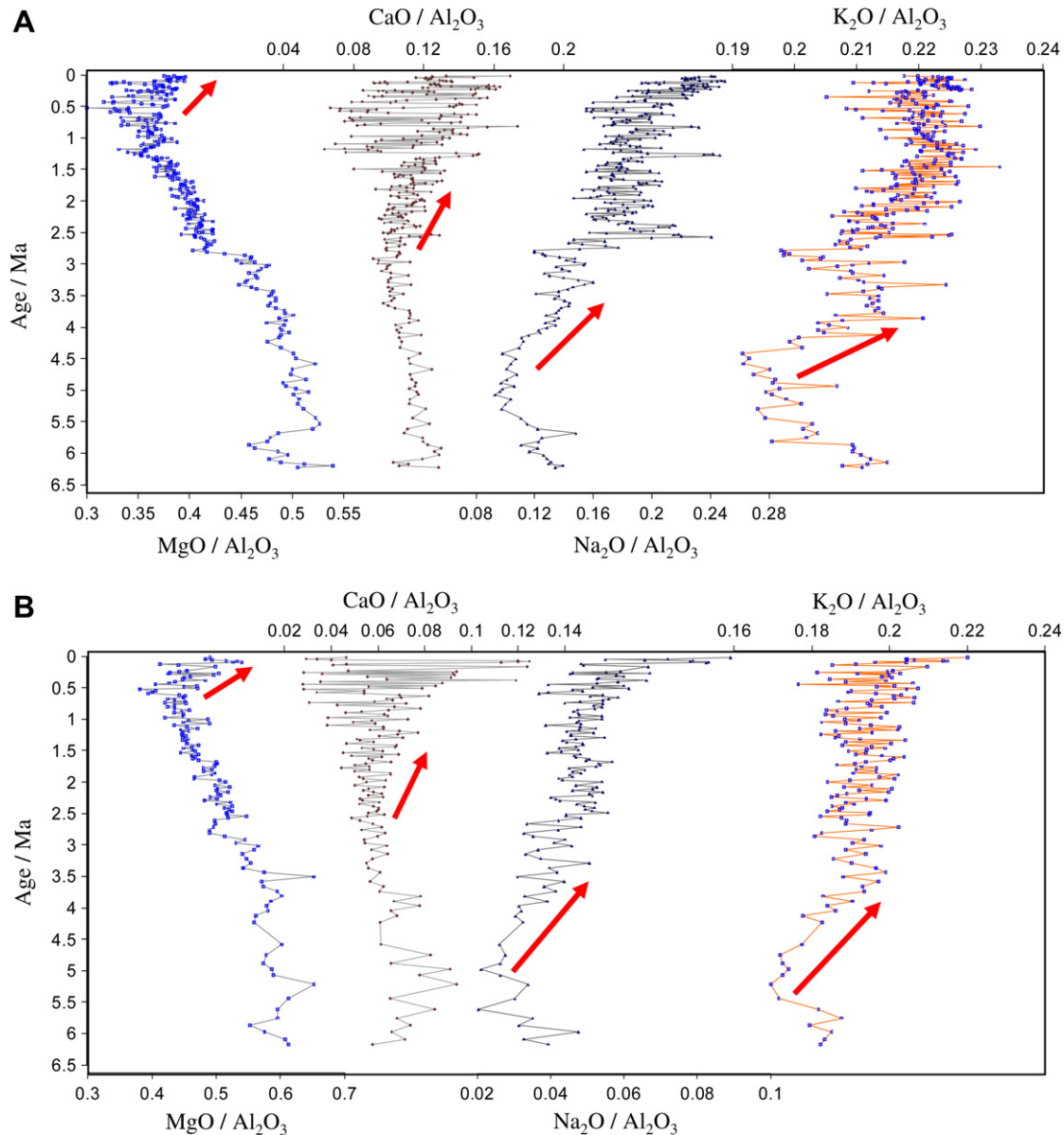
Fig. 10. Variation of MgO/Al$_2$O$_3$, CaO/Al$_2$O$_3$, Na$_2$O/Al$_2$O$_3$ and K$_2$O/Al$_2$O$_3$ ratios for bulk sample (A) and <5 μm size fraction (B) in the Baishui section. Arrows indicate the timing of transitions.

seems that the CIA values of the fine fraction (<5 μm) mainly reflects variations in proportions of various detritus from different sources, and pedogenic alteration only played a minor role.

4.2. The climate-tectonic implications of the chemical evolution of the loess–red clay deposit

The provenance and provenance changes of the Chinese loess–red clay are important subjects for understanding of the relationship between the formation of the loess deposits and regional and global environmental changes. Early work (e.g., Liu et al., 1985; Wen et al., 1989; Liu et al., 1993; Gallet et al., 1996) placed attention on demonstrating the general uniformity in the chemical (isotopic, major and trace elements) composition of Chinese loess. More recently, approaches using different geochemical tracers for individual loess source regions have been pursued (e.g., Sun, 2002; Nakano et al., 2004; Yokoo et al., 2004; Chen et al., 2007; Sun et al., 2007; Yang et al., 2007).

Sun (2002) investigated and compared the isotopic, chemical and mineralogical compositions of the loess in the Loess Plateau and deposits from different deserts, and the results suggested that the gobi in southern Mongolia and the adjoining gobi and sand deserts (the Badain Jaran Desert, Tengger Desert, Ulan Buh Desert, Hobq Desert and Mu Us Desert), rather than the three inland basins (the Junger Basin, the Tarim Basin and the Qaidam Basin), are the main source areas of the Loess Plateau sediments. Yokoo et al. (2004) conducted an analysis for the mineralogical, elemental, and Sr–Nd isotopic compositions of HCl-soluble and -insoluble minerals in the Loess Plateau loess, and found that the loess composition was different from those of the Tengger and Mu Us sand, but were indistinguishable from the fine-grained fraction in these two deserts. Chen et al. (2007) identified three isotopic regions of Chinese deserts based on the Nd–Sr isotopes and suggested that the Nd–Sr isotopic compositions of the loess most closely resemble those of the deserts on the northern margin of Tibetan Plateau, implying that the Badain Jaran Desert, Tengger
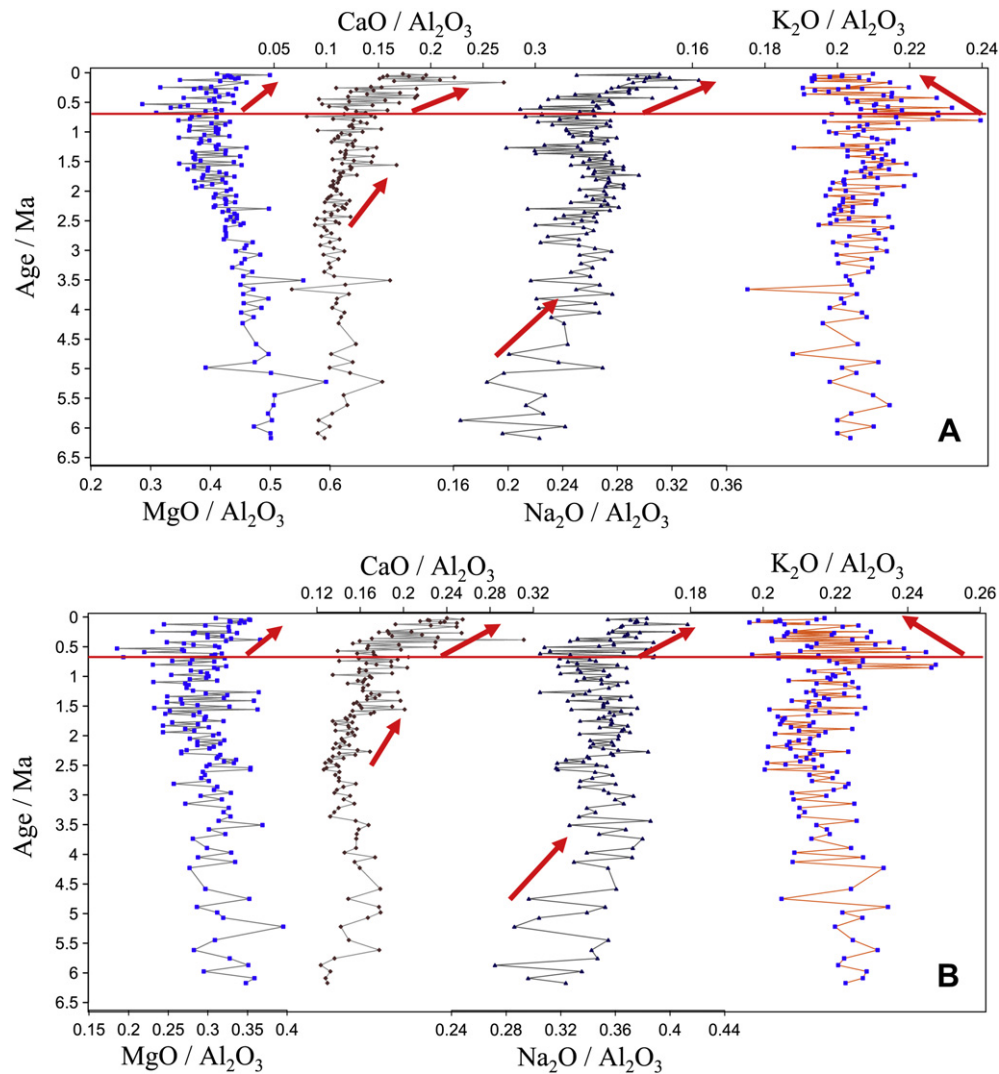
Fig. 11. Variation of MgO/Al$_2$O$_3$, CaO/Al$_2$O$_3$, Na$_2$O/Al$_2$O$_3$ and K$_2$O/Al$_2$O$_3$ ratios for intermediate (5–20 μm) (A) and coarse (20–63 μm) size fraction (B) in the Baishui section. Arrows indicate the timing of transitions. Red line indicates the transition at about 0.6 Ma. (For interpretation of the references to colour in this figure legend, the reader is referred to the web version of this article.)

Desert, and Qaidam Desert, but not the Mu Us Desert, are the main source regions of the last glacial loess in the Loess Plateau. Based on electron spin resonance (ESR) signal intensity and the crystallinity index (CI) of quartz, Sun et al. (2007) differentiated nine Gobi and sandy deserts in China. Analysis of sediments from Lingtai suggested that the Loess Plateau sediment is derived mainly from the Gobi desert in southern Mongolia and the sandy deserts in northern China (primarily the Badain Jaran and Tengger deserts), rather than from the Taklimakan desert, at least during the last climatic cycle (Sun et al., 2008). It seems that most recent studies agree in that the loess source regions are the arid regions in western China, especially the Badain Jaran and Tengger deserts, although the Qaidam desert and Mu Us desert were not included in all studies.

There are very few studies centered on provenance change of the Chinese loess–red clay. Gallet et al. (1996) and Jahn et al. (2001) analyzed Nd and Sr isotopes of bulk samples from the Loess Plateau, and the results suggested that Nd and Sr isotopic compositions of loess–paleosols are rather uniform, implying a uniform source region during loess deposition over the past 800 ka. Sun (2005) investigated the temporal variations of the <20 μm Nd and Sr isotopic compositions of the Jingchuan section in the middle of the

Loess Plateau, and found that Quaternary loess–paleosols exhibit lower values of ^{143}Nd/^{144}Nd ratios than that of the Tertiary Red Clay, with a prominent decrease of ^{87}Sr/^{86}Sr ratios after 2.58 Ma. The author concluded that this shift implies a major change in provenance of the eolian dust around 2.58 Ma ago (Sun, 2005). This interpretation was recently questioned by Wang et al. (2007) because their study of the Lingtai section reveals a generally descending trend of ^{87}Sr/^{86}Sr from 0.7223 at ∼2.5 Ma BP to 0.7182 at the present. The authors attribute this trend to grain size distribution change, rather than provenance or chemical weathering changes (Wang et al., 2007). The analyses of Wang et al. (2007) also reveal that all the red clay and the overlying loess–paleosols in the Lingtai profile have generally identical ϵ_{Nd} (0), and the authors suggested that the source regions of the Chinese Loess Plateau eolian sediments have not changed since 7 Ma BP. According to Wang et al. (2007), the fluctuations of ϵ_{Nd} (0) values in both the Lingtai and Jingchuan profiles are much smaller than 0.7ϵ units, within the range of the experimental error, thus the proposed provenance change of Sun (2005) needs to be reinvestigated.

Although Nd and Sr isotopes studies yield conflicting results concerning the issue of loess provenance changes, recent magnetic
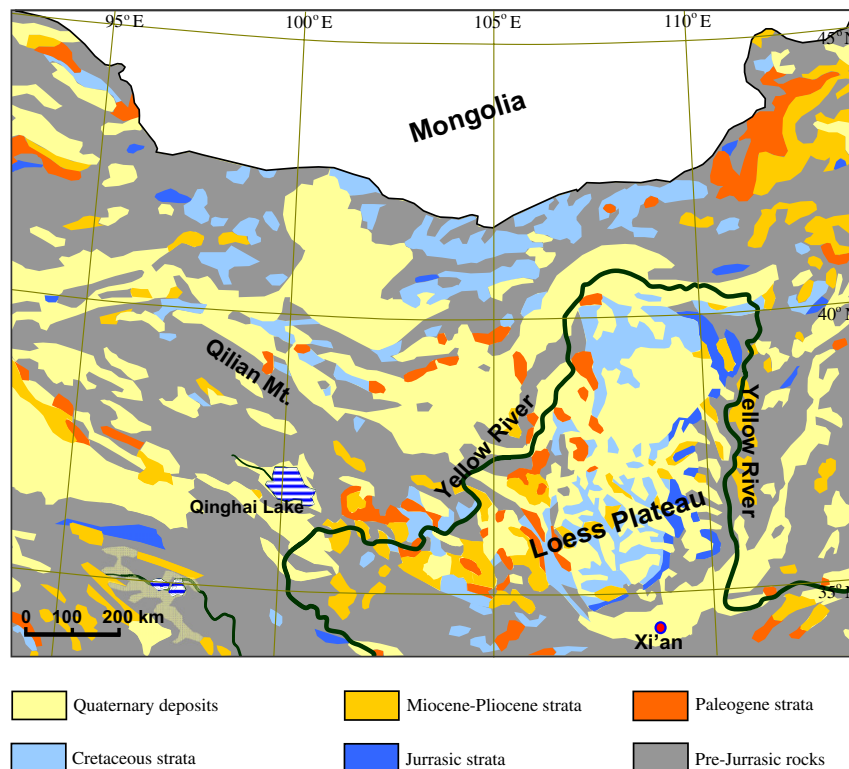
Fig. 12. Geological map showing the distributions of the Jurrasic, Cretaceous and Paleogene strata distributed in the northwestern China, simplified from the Editing Committee of Geological Atlas of China (2002) and the Institute of Geology, Chinese Academy of Geological Sciences and Wuhan College of Geology (1985).

approaches seem to provide another perspective on the question. Rock magnetic analyses of the Jingbian loess section (Deng et al., 2006) showed a long-term up-section decreasing trend in the saturation isothermal remanent magnetization (SIRM) ratios of both loess and paleosol units, and this variation is attributed to a long-term decrease in the relative contribution of eolian hematite during glacial extrema and of pedogenic hematite during interglacial extrema, respectively. Hao et al. (2008) investigated the IRM_{300mT}/IRM_{100mT} ratio of a long eolian sequence and the ratio showed a generally decline over the last 22 Ma that they attributed to changes in the relative proportions of hematite and goethite, variations in grain size or changes in the degree of aluminium substitution. The changing relative proportions of hematite (and perhaps goethite) in the eolian deposits (Deng et al., 2006; Hao et al., 2008) cannot be solely interpreted as variation in weathering intensity because there is no correlation between the magnetic proxies and the pedogenetic strength (for example, glacial–interglacial fluctuations) observed in these deposits. These results may implicate a long-term change in the loess provenance.

Our results provide new insight into the questions of loess provenance change. It is well known that the loess–red clay is essentially a type of detrital deposit and its chemical composition would have been influenced by the sediment composition and weathering regime of the source region(s), sedimentary sorting during erosion, transportation and deposition and pedogenetic alternation after deposition in loess or red clay deposits. By analyzing the chemical composition of size fractions, we hoped to minimize (and differentiate) the influence of sedimentary sorting on the chemical composition of the bulk loess–red clay samples. After comparing size differentiated chemical compositions with several typical deposits in China (Fig. 9) and considering the small amplitudes of CIA values between loess and paleosol horizons, it is estimated that the loess–red clay has experienced incipient to

intermediate chemical weathering and that the pedogenic alterations are less significant than sediment sorting and source area changes in influencing the bulk sediment chemical composition.

The change in slope at about SiO_2 65% in the Harker diagram (bivariate plot of Al_2O_3, FeO_T, K_2O versus SiO_2) for the bulk samples (Fig. 3) suggests a major shift in provenance of the eolian dust at the red clay-loess transition (~ 2.7 Ma). Analysis of the molar ratios of the labile oxides normalized to Al_2O_3 for the bulk and fine component reveals similar chemical evolution for both size fractions. A sequential increase in the background values of K_2O/Al_2O_3, Na_2O/Al_2O_3, CaO/Al_2O_3 and MgO/Al_2O_3 ratios occurs between about 5.5–4.5 Ma to about 0.6 Ma (Fig. 10). For the coarse and intermediate fractions, no apparent transition in the K_2O/Al_2O_3 ratio is observed between 5.5 and 4.5 Ma, but a chemical evolution sequence similar to the bulk and fine fraction samples can be still seen for the Na_2O/Al_2O_3, CaO/Al_2O_3 and MgO/Al_2O_3 ratios from 4.5 Ma to about 0.6 Ma. It is known that the main minerals in the loess–red clay deposits are quartz, plagioclase, K-feldspar, biotite, muscovite and clay minerals (Liu et al., 1985). The variations in the K_2O/Al_2O_3, Na_2O/Al_2O_3, CaO/Al_2O_3 and MgO/Al_2O_3 ratios along the loess–red clay sequence are a result of changes in relative content of these minerals. It seems that from about 4.5 Ma, K-feldspar and Na-rich plagioclase (as well as the weathering product illite) from the source regions (uplifted mountains and sedimentary basins) began to increase in quantity. Ca-silicate (e.g., Ca-rich plagioclase) content may have declined due to the dilution of the new input of K-feldspar and Na-rich plagioclase. From about 2.5 Ma, the CaO/Al_2O_3 ratio increased for the less weathered loess layers, implying an increased input of newly eroded Ca-silicates. The CaO/Al_2O_3 ratio of loess layers increased from 2.5 Ma, while the CaO/Al_2O_3 ratio for paleosol layers decreased, resulting in an amplifying fluctuation of the CaO/Al_2O_3 ratio between loess and paleosols from 2.5 Ma to the present (Fig. 10). The declining MgO/Al_2O_3 ratio toward 0.6 Ma may

reflect changing chlorite concentration due to dilution by other minerals. After 0.6 Ma, the MgO/Al_2O_3 ratio increases, probably due to fresh input of Mg-silicates (including detrital chlorite). This 'variation sequence' of chemical composition in the loess–red clay deposits may be caused by provenance change and/or chemical weathering processes.

From the perspective of provenance change, the sequential chemical evolution of the loess–red clay for the bulk and other size fractions may indicate that the composition of the dust source regions has undergone a progressive change from about 4.5 Ma (or earlier) due to an increase of relatively unweathered eroded detritus. We speculate that during the early Pliocene to Pleistocene, the uplifted terrains (e.g., Tapponnier et al., 2001) and strengthened glacial erosion under global cooling (e.g., Zhang et al., 2001) may have greatly and progressively increased denudation rate in the northern Tibetan regions, and the resultant unroofing of the uplifted mountains surrounding the upwind deserts of the Chinese Loess Plateau may have progressively increased detritus input to the deserts with changing detrital compositions from K-Na-rich minerals to Ca–Mg-rich minerals, which were eventually eroded and transported by winds and deposited as loess–red clay with its sequential variations in composition. On the other hand, the variations in weathering intensity may have also played a role in the observed 'variation sequence' in loess–red clay deposit. The progressive global cooling and regional aridification during the late Miocene and Pliocene may cause subsequent decreasing in chemical weathering strength over arid dust source regions and loess deposition areas in the northwestern China, leaving the 'variation sequence' in chemical compositions of the loess–red clay deposit. It seems that at about 4.5 Ma, 2.6 Ma, and 0.6 Ma there are apparent changes in vegetation over the middle part of the Loess Plateau (Wang et al., 2006; Wu et al., 2007). The correlation between the vegetation change and the chemical composition of loess–red clay suggests a climate link. Thus the 'variation sequence' in chemical composition of loess–red clay may reflect provenance change as well as chemical weathering processes. Differentiating the effect of provenance change and weathering processes on the chemical compositions of loess–red clay remains a difficult task.

5. Conclusions

Chemical (major element) analyses on the bulk samples of Baishui loess–red clay sequence preserve a 6 Ma chemical weathering history. The CIA (chemical index of alteration) values display progressively upward weakening weathering intensity with increasing weathering variation amplitudes, which correlates well with the oxygen isotope variations of the deep sea sediments. Analyses of different sample size fractions (<5 μm, 5–20 μm and 20–63 μm) indicate that CIA and the major element abundances are strongly related with grain size of particles. The chemical alternations of all of the three size fractions are relatively weak, and the long-term trend of the chemical evolution for the loess–red clay is mainly controlled by the input of newly eroded detritus and mixing processes. The patterns of CIA variations for the coarse fractions (5–20 μm and 20–63 μm) along the section are different from those for the fine fraction (<5 μm), implying different weathering and mixing histories for the size fractions. From 1 Ma onward, CIA values for each size fractions of the samples all decrease, implying an increasing input of fresh or poorly weathered detritus into the source regions of loess deposits. Further analyses of the bulk sample and different size fractions display a similar sequence pattern which displays progressive transitions for the K_2O/Al_2O_3, Na_2O/Al_2O_3, CaO/Al_2O_3 and MgO/Al_2O_3 ratios from 4.5 Ma to about 0.6 Ma, and this 'variation sequence' in chemical

composition of loess–red clay may reflect provenance change as well as chemical weathering processes.

Appendix

Supplementary data associated with this article can be found in the online version, at doi:10.1016/j.quascirev.2010.04.009.

References

Chen, J., An, Z., Head, J., 1999. Variation of Rb/Sr ratios in the loess–paleosol sequences of central China during the last 130,000 years and their implications for monsoon paleoclimatology. Quaternary Research 51, 215–219.

Chen, J., Li, G., Yang, J., Rao, W., Lu, H., Balsam, W., Sun, Y., Ji, J., 2007. Nd and Sr isotopic characteristics of Chinese deserts: implications for the provenances of Asian dust. Geochimica et Cosmochimica Acta 71, 3904–3914.

Chen, L., Li, F.X., Di, X.M., Zhang, W., 1998. Aeolian Sandy Soils in China. Science Press, Beijing (in Chinese).

Chittleborough, D.J., 1991. Indices of weathering for soil and paleosols formed on silicate rocks. Australian Journal of Earth Sciences 38, 115–120.

Deng, C., Shaw, J., Liu, Q., Pan, Y., Zhu, R., 2006. Mineral magnetic variation of the Jingbian loess/paleosol sequence in the northern Loess Plateau of China: implications for Quaternary development of Asian aridification and cooling. Earth and Planetary Science Letters 241, 248–259.

Ding, Z.L., Yu, Z.W., Rutter, N.W., Liu, T., 1994. Towards an orbital time scale for Chinese loess deposits. Quaternary of Science Reviews 13, 39–70.

Ding, Z.L., Xiong, S.F., Sun, J.M., Yang, S.L., Gu, Z.Y., Liu, T.S., 1999. Pedostratigraphy and paleomagnetism of a ~7.0 Ma eolian loess–red clay sequence at Lingtai, Loess Plateau, north-central China and the implications for paleomonsoon evolution. Palaeogeography, Palaeoclimatology, Palaeoecology 152, 49–66.

Ding, Z.L., Yang, S.L., Hou, S.S., Wang, X., Chen, Z., Liu, T.S., 2001a. Magneto-stratigraphy and sedimentology of the Jingchuan red clay section and correlation of the Tertiary eolian red clay sediments of the Chinese Loess Plateau. Journal of Geophysical Research 106 (B4), 6399–6407.

Ding, Z.L., Yang, S.L., Sun, J.M., Liu, T.S., 2001b. Iron geochemistry of loess and red clay deposits in the Chinese Loess Plateau and implications for long-term Asian monsoon evolution in the last 7.0 Ma. Earth and Planetary Science Letters 185, 99–109.

Ding, Z.L., Sun, J.M., Yang, S.L., Liu, T.S., 2001c. Geochemistry of the Pliocene red clay formation in the Chinese Loess Plateau and implications for its origin, source provenance and paleoclimate change. Geochimica et Cosmochimica Acta 65, 901–913.

Dixon, J.B., Weed, S.B. (Eds.), 1989. Minerals in Soil Environments, second ed. Soil Science Society of America, Madison.

Editing Committee of Geological Atlas of China, 2002. Geological Atlas of China. Geological Publishing House, Beijing, 348 pp.

Gallet, S., Jahn, B.-M., Torii, M., 1996. Geochemical characterization of the Luochuan loess–paleosol sequence, China, and paleoclimatic implications. Chemical Geology 133, 67–88.

Gallet, S., Jahn, B.-M., Van Vliet Lanoe, B., Dia, A., Rossello, E., 1998. Loess geochemistry and its implications for particle origin and composition of the upper continental crust. Earth and Planetary Science Letters 156, 157–172.

Gu, Z.Y., Ding, Z., Xiong, S., Liu, T., 1999. A seven million geochemical record from Chinese red clay and loess–paleosol sequence: weathering and erosion in northwestern China. Quaternary Science 19, 357–365 (in Chinese with English abstract).

Guo, Z.T., Biscaye, P., Wei, L.Y., Chen, X.H., Peng, S.Z., Liu, T.S., 2000. Summer monsoon variations over the last 1.2 Ma from the weathering of loess-soil sequences in China. Geophysical Research Letters 27, 1751–1754.

Guo, Z.T., Ruddiman, W.F., Hao, Q.Z., Wu, H.B., Qiao, Y.S., Zhu, R.X., Peng, S.Z., Wei, J.J., Yuan, B.Y., Liu, T.S., 2002. Onset of Asian desertification by 22 Myr ago inferred from loess deposits in China. Nature 416, 159–163.

Gylesjo, S., Arnold, E., 2006. Clay mineralogy of a red clay-loess sequence from Lingtai, the Chinese Loess Plateau. Global and Planetary Change 51, 181–194.

Hao, Q., Oldfield, F., Bloemendal, J., Guo, Z., 2008. The magnetic properties of loess and paleosol samples from the Chinese Loess Plateau spanning the last 22

million years. Palaeogeography, Palaeoclimatology, Palaeoecology 260, 389–404.

Harnois, L., 1988. The CIW index: a new chemical index of weathering. Sedimentary Geology 55, 319–322.

Institute of Geology, Chinese Academy of Geological Sciences, Wuhan College of Geology, 1985. Atlas of the Palaeogeography of China. Cartographic Publishing House, Beijing (in Chinese).

Jahn, B.-M., Gallet, S., Han, J., 2001. Geochemistry of the Xining, Xifeng and Jixian sections, Loess Plateau of China: eolian dust provenance and paleosol evolution during the last 140 ka. Chemical Geology 178, 71–94.

Liu, C.Q., Masuda, A., Okada, A., Yabuki, S., Zhang, J., Fan, Z.L., 1993. A geochemical study of loess and desert sand in northern China: implications for continental crust weathering and composition. Chemical Geology 106, 359–374.

Liu, T.S., et al., 1965. The Loess Deposits of China. Science Press, Beijing (in Chinese).

Liu, T.S., et al., 1966. The Composition and Texture of Loess. Science Press, Beijing (in Chinese).

Liu, T.S., et al., 1985. Loess and the Environment. Chinese Ocean Press, Beijing.

Maslin, M.A., Haug, G.H., Sarnthein, M., Tiedemann, R., 1996. The progressive intensification of northern hemisphere glaciation as seen from the North Pacific. Geologische Rundschau 85, 452–465.

Mix, A.C., Pisias, N.G., Rugh, W., Wilson, J., Morey, A., Hagelberg, T.K., et al., 1995. Benthic foraminifer stable isotope record from Site 849 (0–5 Ma): local and global climate changes. In: Pisias, N.G., Mayer, L.A., Janecek, T.R. (Eds.), Proceedings of the Ocean Drilling Program, Scientific Results, vol. 138. Ocean Drilling Program, College Station, TX, pp. 371–412.

Nakano, T., Yokoo, Y., Nishikawa, M., Koyanagi, H., 2004. Regional Sr-Nd isotopic ratios of soil minerals in northern China as Asian dust fingerprints. Atmospheric Environment 38, 3061–3067.

Nesbitt, H.W., Young, G.M., 1982. Early Proterozoic climates and plate motions inferred from major element chemistry of lutites. Nature 299, 715–717.

Nesbitt, H.W., Young, G.M., McLennan, S.M., Keays, R.R., 1996. Effects of chemical weathering and sorting on the petrogenesis of siliciclastic sediments, with implications for provenance studies. Journal of Geology 104, 525–542.

Parker, A., 1970. An index of weathering for silicate rocks. Geological Magazine 107, 501–504.

Raymo, M.E., 1994. The initiation of Northern Hemisphere glaciation. Annual Reviews of Earth and Planetary Sciences 22, 353–383.

Rollinson, H., 1993. Using Geochemical Data: Evolution, Presentation, Interpretation. Longman, Harlow.

Ruxton, B.P., 1968. Measures of the degree of chemical weathering of rocks. Journal of Geology 76, 518–527.

Shackleton, N.J., Hall, M.A., Pate, D., et al., 1995. Pliocene stable isotope stratigraphy of Site 846. In: Pisias, N.G., Mayer, L.A., Janecek, T.R. (Eds.), Proceedings of the Ocean Drilling Program, Scientific Results, vol. 138. Ocean Drilling Program, College Station, TX, pp. 337–355.

Smalley, I.J., 1995. Making the material: the formation of silt-sized primary mineral particles for loess deposits. Quaternary Science Reviews 14, 645–651.

Sun, J., 2002. Provenance of loess material and formation of loess deposits on the Chinese Loess Plateau. Earth and Planetary Science Letters 203, 845–859.

Sun, J., 2005. Nd and Sr isotopic variations in Chinese eolian deposits during the past 8 Ma: implications for provenance change. Earth and Planetary Science Letters 240, 454–466.

Sun, Y., Tada, R., Chen, J., Chen, H., Toyoda, S., Tani, A., Isozaki, Y., Nagashima, K., Hasegawa, H., Ji, J., 2007. Distinguishing the sources of Asian dust based on electron spin resonance signal intensity and crystallinity of quartz. Atmospheric Environment 41, 8537–8548.

Sun, Y., Tada, R., Chen, J., Liu, Q., Toyoda, S., Tani, A., Ji, J., Isozaki, Y., 2008. Tracing the provenance of fine-grained dust deposited on the central Chinese Loess Plateau. Geophysical Research Letters 35, L01804. doi:10.1029/2007GL031672.

Tapponnier, P., Xu, Z.Q., Roger, F., Meyer, B., Arnaud, N., Wittlinger, G., Yang, J.S., 2001. Oblique stepwise rise and growth of the Tibet Plateau. Science 294, 1671–1677.

Taylor, S.R., McLennan, S.M., McCulloch, M.T., 1983. Geochemistry of loess, continental crustal composition and crustal model ages. Geochimica et Cosmochimica Acta 47, 1897–1905.

Vogel, D.E., 1975. Precambrian weathering in acid metavolcanic rocks from the Superior Province, Villebon Township, South-Central Quebec. Canadian Journal of Earth Sciences 12, 2080–2085.

Vogt, T., 1927. Sulitjelmafeltets geologi og petrografi. Norges Geologiske Undersokelse 121, 1–560.

Wang, L., Lu, H.Y., Wu, N.Q., Li, J., Pei, Y.P., Tong, G.B., Peng, S.Z., 2006. Palynological evidence for Late Miocene-Pliocene vegetation evolution recorded in the red clay sequence of the central Chinese Loess Plateau and implication for palaeoenvironmental change. Palaeogeography, Palaeoclimatology, Palaeoecology 241, 118–128.

Wang, Y.X., Yang, J.D., Chen, J., Zhang, K.J., Rao, W.B., 2007. The Sr and Nd isotopic variations of the Chinese Loess Plateau during the past 7 Ma: implications for the East Asian winter monsoon and source areas of loess. Palaeogeography, Palaeoclimatology, Palaeoecology 249, 351–361.

Wen, Q.Z., et al., 1989. Loess Geochemistry in China. Science Press, Beijing (in Chinese).

Wright, J.S., 2001. "Desert" loess versus "glacial" loess: quartz silt formation, source areas and sediment pathways in the formation of loess deposits. Geomorphology 36, 231–256.

Wu, F., Fang, X., Ma, Y., Herrmann, M., Mosbrugger, V., An, Z., Miao, Y., 2007. Plio-Quaternary stepwise drying of Asia: evidence from a 3-Ma pollen record from the Chinese Loess Plateau. Earth and Planetary Science Letters 257, 160–169.

Xiong, S.F., Ding, Z.L., Liu, T.S., 2001. Mass balance geochemistry of the red earth in southern China and its environmental implications. Acta Pedologica Sinica 38, 25–31.

Xiong, S.F., Jiang, W.Y., Yang, S.L., Ding, Z.L., Liu, T.S., 2002. Northwestward decline of magnetic susceptibility for the red clay deposit in the Chinese Loess Plateau. Geophysical Research Letters 29, 2162. doi:10.1029/2002GL015808.

Xiong, S.F., Ding, Z.L., Jiang, W.Y., Yang, S.L., Liu, T.S., 2003. Initial intensification of East Asian winter monsoon at about 2.75 Ma as seen in the Chinese eolian loess–red clay deposit. Geophysical Research Letters 30, 1524. doi:10.1029/2003GL017059.

Xiong, Y., Li, Q.K. (Eds.), 1987. Soils of China. Science Press, Beijing (in Chinese).

Yang, X., Liu, Y., Li, C., Song, Y., Zhu, H., Jin, X., 2007. Rare earth elements of aeolian deposits in Northern China and their implications for determining the provenance of dust storms in Beijing. Geomorphology 87, 365–377.

Yang, S.L., Ding, F., Ding, Z.L., 2006. Pleistocene chemical weathering history of Asian arid and semi-arid regions recorded in loess deposits of China and Tajikistan. Geochimica et Cosmochimica Acta 70, 1695–1709.

Yokoo, Y., Nakano, T., Nishikawa, M., Quan, H., 2004. Mineralogical variation of Sr–Nd isotopic and elemental compositions in loess and desert sand from the central Loess Plateau in China as a provenance tracer of wet and dry deposition in the northwestern Pacific. Chemical Geology 204, 45–62.

Zachos, J., Pagani, M., Sloan, L., Thomas, E., Billups, K., 2001. Trends, rhythms, and aberrations in global climate 65 Ma to present. Science 292, 686–693.

Zhang, P.Z., Molnar, P., Downs, W.R., 2001. Increased sedimentation rates and grain sizes 2–4 Myr ago due to the influence of climate change on erosion rates. Nature 410, 891–897.